Special edition paper

Basic Study on Shear Failure Behavior by Shear Rebar Used as Seismic Reinforcement of Underground RC Structures


Kaoru Kobayashi*


Hideaki Takano*


Naomi Sasaki*

In order to provide underground RC structures with seismic reinforcement, JR East is developing a construction method whereby shear rebars are added from drilled holes because the ground around the structure prevents reinforcement from outside. One possible method of installing shear rebars to underground RC structures afterward at low cost is to use large-diameter rebars. However, this method requires careful consideration of the anchorage length and shear reinforcement effect if such large-diameter rebars are used. Assuming use of large-diameter rebars for wall members, we studied failure behavior based on shear failure tests using beam specimens at their actual cross-section height and three-dimensional nonlinear FEM analysis. The results clarified that failure occurs and develops due to bond deterioration at the end of large-diameter rebars.

●Keywords: Underground RC structure, Seismic reinforcement, Shear reinforcement

1 Introduction

Work on reinforcement of concrete structures has been active since the 1995 Great Hanshin-Awaji Earthquake. Recently, examples of seismic reinforcement of underground reinforced concrete (RC) structures have been reported.[1] Underground RC structures are surrounded by ground, so seismic reinforcement from inside using drilled holes is assumed to be reasonable, as is shown in some studies.[2)-6)]

When providing seismic reinforcement to underground RC structures, the main aim is shear reinforcement of members. If reinforcement work is done from inside, the member to be reinforced is drilled, shear rebars are inserted, and then the member is filled with grout or the like so that the shear rebar and the member are sufficiently integrated to each other. In such post-construction installation, the shear reinforcement is bar shaped. In past studies on the use of shear rebars, researchers have focused on shear performance with[2)-4)] and without[5), 6)] anchorage at the end of the rebar to shorten the anchorage length.

In those studies,[2)-6)] the researchers used specimens with a cross-section height (h) of 340 to 1,000 mm, effective height (d) of 300 to 905 mm, and diameter of shear rebar used (ø) of D10 (SD295) to D22 (SD345). In reference document 3, the researchers used PC steel bars of ø13 mm (SBPR1080/1230) and ø17 mm (SBPR1080/1230). In those past studies, researchers disregarded whether the shear rebars had anchorage at their end or not. The ratio of half the effective height (d) and the rebar diameter was 9.4 to 26.6, showing that the tests were often carried out using rebars with relatively long anchorage.

For cost reduction of seismic reinforcement of underground RC structures, using rebars of as large a diameter as possible so as to the number of the rebars is assumed to be effective.

In light of that, we carried out experimental examination of post-construction installation of shear reinforcement for underground RC structures with a view of applying large-diameter rebars. The specimens used were RC beams of a height (h) of 700 mm, effective height (d) of around 600 mm and cross-section height of roughly equal to that of the actual culvert. For the shear rebar, we used D25 (SD345) and D38 (SD390). The ratios of half the effective height (d) and the rebar diameter (ø) were 8.4 and 12.0. The experiment results showed that the difference of the diameter of the shear rebar leads to different modes of failure, even when the amounts of shear reinforcement of the specimens are roughly equal to each other. Specifically, flexural failure occurred with the specimen using D25 (SD345), while compressive shear failure occurred with the specimen using D38 (SD390).

Based on those results, we focused on the failure mechanism when using D38 (SD390) large-diameter rebar as shear reinforcement. In that, we considered seismic reinforcement of underground RC structures in three-dimensional nonlinear FEM analysis and the like.

2 Outline of Destructive Tests

2.1 Details of the Specimens

Table 1 shows the specifications of the specimens, and Fig. 1 shows their shapes.

We used three test specimens of the cross-sectional dimensions 420 mm × 700 mm. The cross-section height was 700 mm and the effective height around 600 mm, similar to the height of members for ordinary culverts. The shear span was 1,900 mm and the shear span ratio (la/d) around 3.0. Each of the three specimens failed on the side from the loading point to the movable support point and was reinforced on the side from loading point to the fixed support point. As reinforcement, D16 (SD345) shear rebars were placed at intervals of 100 mm to prevent shear failure. The object of this experiment was to clarify the shear failure area.

Case-1 was a basic specimen without shear reinforcement. Case-2 was a specimen with D25 shear rebars in two rows at intervals of 300 mm. The 300 mm interval was decided as around a half of the effective height (d), the maximum interval of shear rebars stipulated in design standard and the like for RC structures.

For Case-2, D25 shear rebars were used. We split a rebar in two lengthwise and milled a slot on each of the rebar halves to attach a strain gauge inside. We then bonded that rebar to

*Frontier Service Development Laboratory, Research and Development Center of JR East Group

Table 1 List of the Specimens

Specimen name	Cross-section width B(mm)	Cross-section height D(mm)	Cross-section effective height d(mm)	Span L(mm)	Shear span la(mm)	Shear span ratio la/d	Main rebar diameter	Main rebar steel standard	Shear rebar	Shear rebar standard	Shear rebar shape	Shear rebar interval (mm)	Concrete strength f'ck(N/mm^2)
Case-1	420	700	603	4300	1900	3.15	D32	SBPD930 /1080	None	—	—	—	22.3
Case-2	420	700	603	4300	1900	3.15	D32	SBPD930 /1080	Two half D25 rebars bonded together placed in two rows	SD345	Bar	300	20.8
Case-3	420	700	635	4300	1900	2.99	D32	SBPD930 /1080	D38 placed in a row	SD390	Bar	300	25.7
									One set of D-6	SD345	Closing	600	

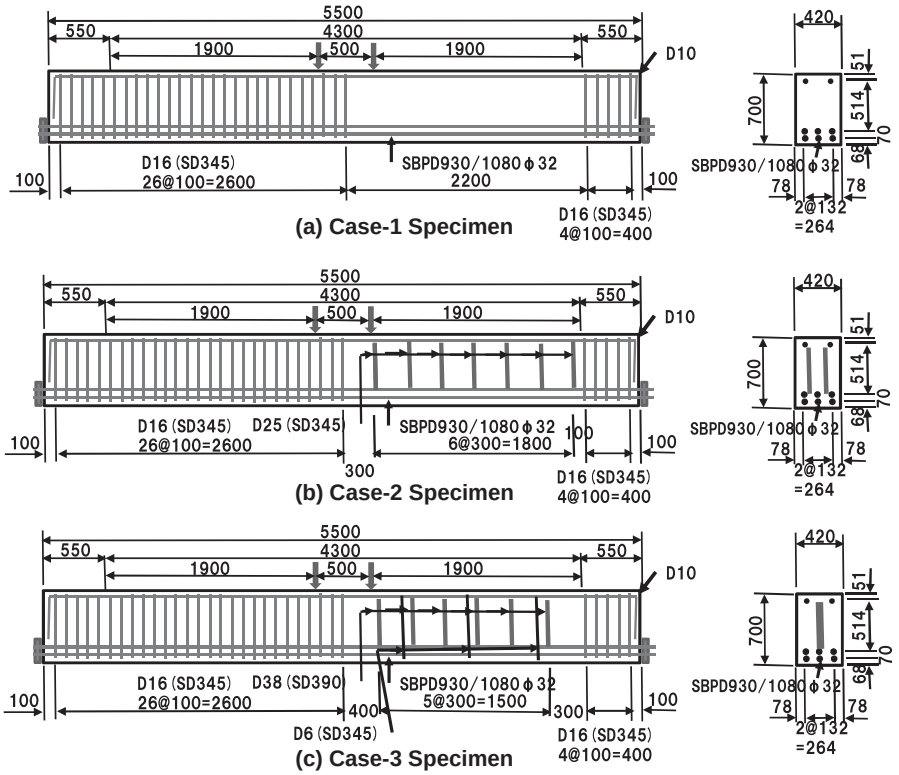

Fig. 1 Detailed Diagrams of Specimens

another D25 rebar of the same lot that was split in the same manner to make a single shear rebar. Fig. 2 shows a processing drawing of the D25 shear rebars used for the Case-2 specimen. (a) in the figure is the processing dimensions, (b) is the cross-section of the bonded rebar, and (c) is the entire length. Fig. 3 is a photo of the rebar being processed.

We attached a strain gauge to D25 shear rebars in the above-mentioned method so as to maintain the adhesiveness of the rebar to concrete. From a view of production management, we measured the weight of the D25 rebars before processing and calculated the weight per unit volume of individual rebars from the measured weight and the volume based on the nominal cross-sectional area and length of the rebars. The cross-sectional area of the processed shear rebar was 547.3 mm^2, the yield strength 205.4 kN (yield strain of 2016 μ), and the tensile strength 282.2 kN. The cross-sectional area was 1.08 times larger, the yield strength 1.10 times larger, and the tensile strength 1.04 times larger than that of the base rebar.

Case-3 was a specimen with D38 (SD390) shear rebars placed in a row at intervals of 300 mm and D6 (SD345) closing shear rebars placed at intervals of 600 mm. We chose D6 rebars as they are distributing bars of small cross-section so as to minimize

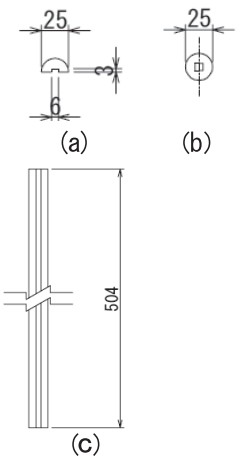

Fig. 2 Production Drawing of D25 Rebar

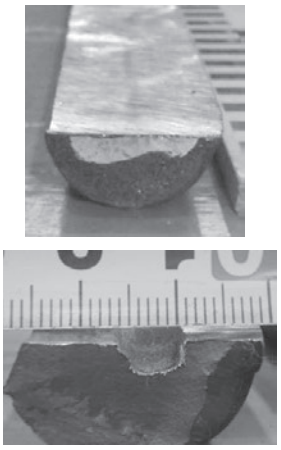

Fig. 3 Processed D25 Rebar

their influence on the tests. The D38 shear rebars were placed at the middle of the width of the cross-section. Their length was 560 mm, which is the interval length between the upper side of the main rebar and the D6 longitudinal rebar on the compressive side. In the mechanical characteristics of D38 rebar, the yield stress was 405.7 N/mm^2 (yield strain of 2,372 μ) and the tensile

strength 612.5 N/mm^2. A strain gauge was attached after the knot on the surface of the rebar was grinded.

The strength of the concrete used for the specimens was 20.8 to 25.7 N/mm^2. Concrete was cast after shear rebars were placed.

2.2 Testing Method

Fig. 4 shows testing being performed. The tests were bending tests at four points. The load was removed until near zero when flexural cracking was visually observed, and then it was gradually applied again to around 50 kN until the specimens being broken. The purpose of removing the load once when flexural cracking occurred was to check the fitting level of the loading plate and the support plates.

2.3 Outline of Measuring for Strain of Shear Rebars

Dividing the entire length of the rebar in four, we attached a strain gauge at the middle of the entire length and at the upper and lower 1/4L from the middle.

3 Overview of Test Results

3.1 Failure Behavior

(1) Case-1 specimen (base specimen)

With Case-1, flexural cracking occurred at the edge of the area of uniform bending with loading of 231 kN. Then, as the load increased, the number of the flexural cracks also increased. With around 350 kN loading, cracking at approx. 700 mm from the loading point in the direction of the support point (at the point about 1.2 times of the effective height d) changed to diagonal cracking. With 450 kN loading, diagonal cracking that started from the point approx. 950 mm from the loading point in the direction to the support point (at a point about 1.58 times effective height d) extended to a point approx. 200 mm from the upper edge. With around 480 kN loading, the diagonal cracking reached the vicinity of the loading point, and as soon as the 485 kN maximum load was recorded, the diagonal cracking went through near the supporting point and the load sharply dropped.

Fig. 5 shows the failure of Case-1. As we found no compressive failure of concrete around the loading point, we determined the failure mode to be diagonal tensile failure.

(2) Case-2 specimen (D25 rebars in two rows at 300 mm intervals)

With Case-2, flexural cracking occurred at the edge of the area of uniform bending with loading of 200 kN. With 500 kN loading, cracking at approx. 600 mm from the loading point in the direction to the support point (at a point approx. 1.0 times effective height d) developed into diagonal cracking.

With 600 kN loading, the cracking at approx. 600 mm, 800 mm, 1,100mm, and 1,300 mm from the loading point to the direction of the support point developed into diagonal cracking. With 750 kN loading, the end of the diagonal cracking that started from the point approx. 1,000 mm from the loading point in the direction to the support point reached a point approx. 80 mm from the upper edge. As the load increased and exceeded 800 kN, cracking in the longitudinal direction of the specimen occurred near the upper surface of the longitudinal rebars. With further loading, the cracking along the longitudinal bar changed its direction, at the support point to the upper edge of the uniform bending area, and then the concrete near the upper edge of the uniform bending area was crushed. The load at crushing was 892 kN.

The diagonal cracking that extended close to the upper edge was almost completely stopped by the longitudinal cracking, and it looked closed at the end. We determined the failure mode of Case-2 to be flexural failure because the cracks that bypassed the shear rebars and entered the uniform bending area caused crushing of the concrete on the upper edge. Fig. 6 shows the failure of Case-2.

(3) Case-3 specimen (D38 (SD390) rebars in a row at 300 mm intervals and D6 (SD345) closing rebars at 600 mm intervals)

With Case-3, flexural cracking occurred with 140 kN loading. With around 300 kN loading, flexural cracking that started from the point approx. 600 mm from the loading point in the direction to the support point (at a point approx. 1.0 times effective height d) turned into diagonal cracking. With 400 kN loading, the flexural cracking at the lower edge approx. 450 mm, 500 mm, 750 mm, and 1,250 mm from the loading point in the direction to the support point turned into diagonal cracking. With 500 kN loading, the end of the diagonal cracking that started from a point approx. 1,250 mm from the loading point in the direction of the support point extended to the point approx. 50 mm from the upper edge. As the load was increased to 600 kN, the end of the diagonal cracking reached a point approx. 50 mm from the upper edge. Then, development of cracking that reached the neighborhood of the upper edge almost completely stopped even with further loading, while development of other diagonal cracking was observed.

With 800 kN, the diagonal cracking that started from the point approx. 750 mm from the loading point in the direction of

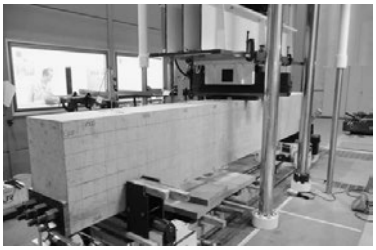

Fig. 4 Loading Test

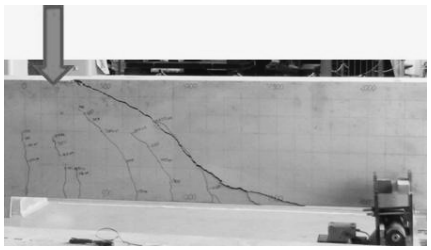

Fig. 5 Failure of Case-1

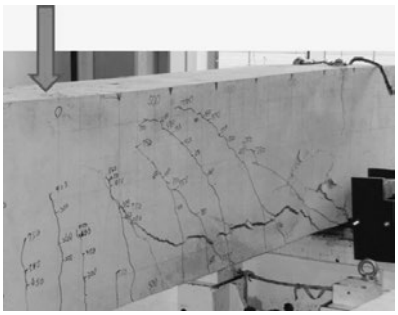

Fig. 6 Failure of Case-2

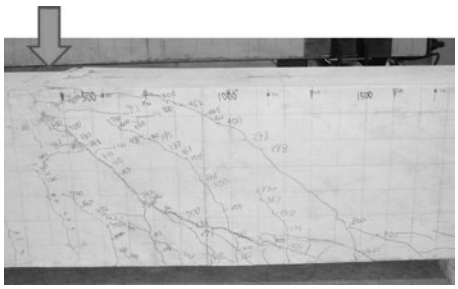

Fig. 7 Failure of Case-3

the support point extended in the direction of the loading point. As loading continued, the upper edge near the loading point was crushed, and the load dropped.

Fig. 7 shows the failure of Case-3. As the cracking that started from a point approx. 750 mm from the loading point extended close to the loading point and the load capacity of the specimen was lost with crushing of the upper edge concrete, we determined the failure mode to be compressive shear failure.

3.2 Load-Deflection Relationships

Fig. 8 (a) to (c) show the load-deflection curves of the three specimens as test results. The load-deflection curves of the analysis results, which will be explained later in Chapter 4, are also shown in the figure. The load is the full weight at the loading point, and the deflection is the perpendicular deflection at the middle of the span. The perpendicular deflection at the middle of the span at which the maximum load was recorded was 5 mm with Case-1 (basic specimen), 20 mm with Case-2 in which flexural failure occurred, and 30 mm with Case-3 in which compressive shear failure occurred.

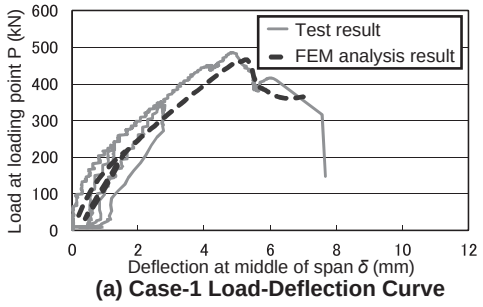

(a) Case-1 Load-Deflection Curve

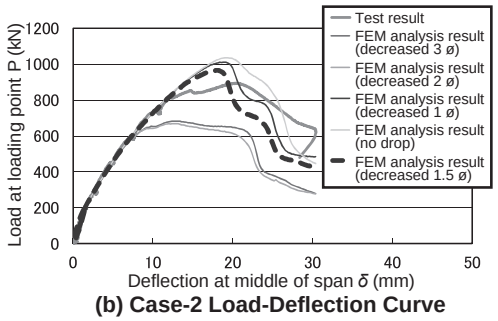

(b) Case-2 Load-Deflection Curve

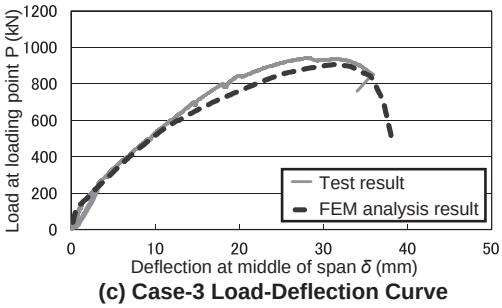

(c) Case-3 Load-Deflection Curve

Fig. 8 Load-Deflection Curves of Individual Test Specimens

3.3 Occurrence of Strain on Shear Rebars

Fig. 9 shows the occurrence of strain on the shear rebars of Case-2 and Fig. 10 shows that of Case-3. In Fig. 9 and 10, the horizontal axis is the strain of the shear rebars and the vertical axis is the load at the loading point.

With the Case-2 specimen using D25 (SD345) shear rebars, the strain on those rebars located within 900 mm from the middle of the span was around 700 to 800 μ (rebars (1) to (3)). The strain on the rebar at 1,200 mm from the middle of the span (rebar (4)) was 500 μ with maximum loading, and it reached the yield strain when the load dropped to 75% of the maximum load. The maximum strain on that rebar reached as high as 4,000 μ.

With the Case-3 specimen using D38 (SD390) shear rebars, the maximum strain on those rebars was around 1,200 μ. This was measured with a strain gauge attached to the middle of that rebar at 700 mm from the middle of the span (rebar (2): at 400 mm from the loading point). As the yield strain on D38 (SD390) rebar is 2,372 μ, about half of the yield strain occurred.

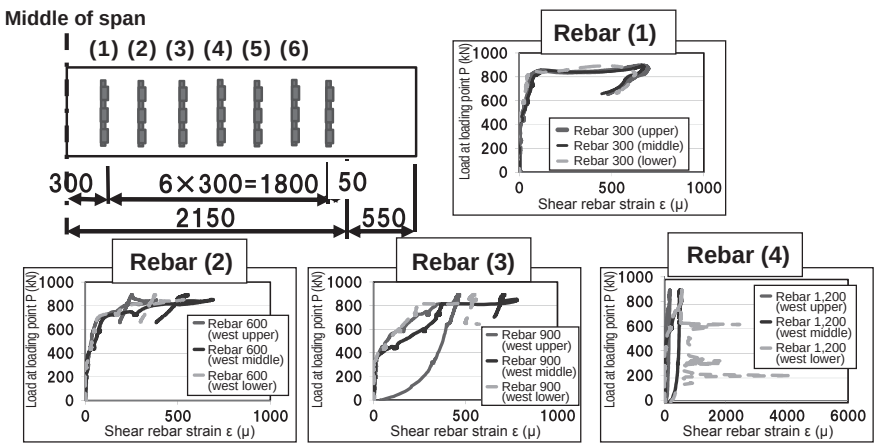

Fig. 9 Occurrence of Strain in Case-2 Specimen Shear Rebars

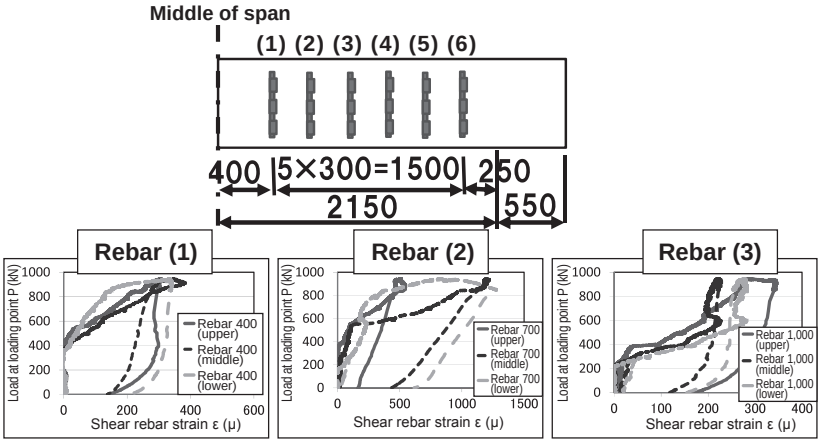

Fig. 10 Occurrence of Strain in Case-3 Specimen Shear Rebars

4 Study of the Failure Mechanism by 3D Nonlinear FEM Analysis

In order to study the shear failure properties of individual specimens, we carried out three-dimensional (3D) nonlinear FEM analysis.

4.1 Overview of the Analysis Model

Fig. 11 shows the analysis model used in this analysis. Based on the symmetry, we applied a half-scale model. The applied constitutive law was the 3D extended RC planar model. The original RC planar model was based on the material composition model that took into account arbitrary loading path dependency, which was developed by the concrete laboratory of the University of Tokyo.

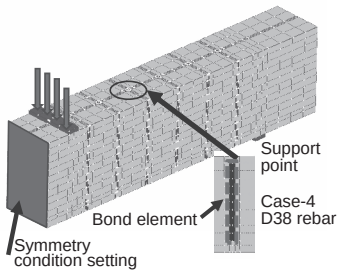

Fig. 11 FEM Analysis Model

(1) Overview of Case-2 specimen analysis model

In analysis of Case-2, how we took into account anchorage of the shear rebars was important. In instances where the end of each rebar was not sufficiently anchored, a method proposed in a past study[8] assumed the rebar ineffective area to be a length equal to 10 times that of the rebar diameter as the effect of such insufficient anchorage.

In this analysis, we conducted analytical studies using the rebar ineffective area (where the rebar ratio within the element was zero) as the parameter. In it, we identified the rebar ineffective area by checking the consistency with the test results, and finally we determined the failure mechanism based on those results.

(2) Overview of Case-3 specimen analysis model

In analysis of Case-3, we placed D38 shear rebars as the rebar elements. Around the D38 rebars, we placed bond elements that expressed properties of bonding to concrete. The bond strength of those bond elements was the calculated value of the bond strength formula indicated in the reference documents[9]. To check the bond behavior of the rebars with bond elements, we first conducted analysis by making the rebar placement the same as that of Case-3 and varying anchorage length of the rebars. The anchorage lengths were 7.5 times, 4.5 times, and 3.0 times the rebar diameter (ø) respectively. For analysis, we applied forced deflection from the upper end of the rebar elements. Deflection was around the volume of dimensionless yield slippage (dimensionless slippage at the time of rebar yield of 0.03, pullout displacement of 1.0 mm) based on the reference documents.[10] The tensile strength at yielding for the D38 (SD390) rebars used for the Case-3 specimen was 465.2 kN; but with the anchorage length of 7.5 ø, remarkable slippage between the rebars and concrete was observed at around 220 kN, about half of the rebar yield strength. Taking into account that the strain of D38 rebars obtained in the tests was around a half of their yield strain, we judged the bond properties of the rebar were largely appropriate, so we used those results in the analysis.

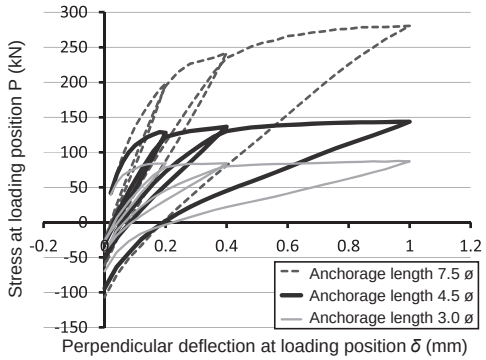

Fig. 12 Bond Properties Given to D38 Rebars

4.2 Analysis Results

(1) Comparison of load-deflection curves

Fig. 8 (a) to (c) are the load-deflection curves from the analysis results.

The analysis results of the Case-2 specimen with a rebar ineffective area of 1.5 ø indicates relatively good consistency to the actual test results. With the Case-3 specimen, overall analysis results were well consistent to the test results.

5 Study of Failure Behavior

Fig. 13 shows the principal strain distribution of the analysis results of the Case-2 specimen just before and at around the maximum load. As the analysis shows, diagonal cracking occurred followed by cracking along the main rebar. And then failure shifted to the upper edge above the middle of the span, resulting in flexural failure.

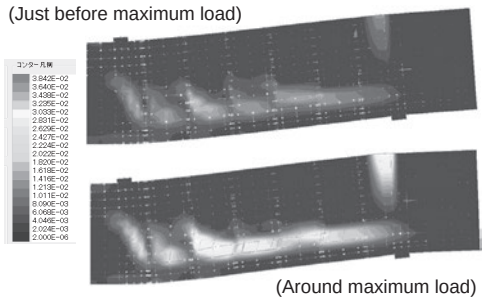

Fig. 13 Results of Case-2 Specimen Failure Behavior Analysis

Fig. 14 (a) and (b) show the principal strain distribution as the analysis results of the Case-3 specimen. Fig. 14 is the analysis results of the side surface and of the middle of the cross-section surface where rebars were located. As shown in Fig. 14 (a), just before the maximum load, the bond at the lower end of the D38 rebars (near the longitudinal rebars) began to be lost. As shown in Fig. 14 (b), at around the maximum load, the D38 rebar slipped at its upper end near the loading point, increasing the principal strain at the upper edge, and finally concrete was crushed. At that time, upper edge concrete was not yet crushed on the side surface. Further increase of deflection enlarged the crush area of the upper edge concrete, causing sharp decrease of the load. Based on those analysis results, we concluded that the slippage of large-diameter rebars at their end caused crushing of the Case-3 specimen.

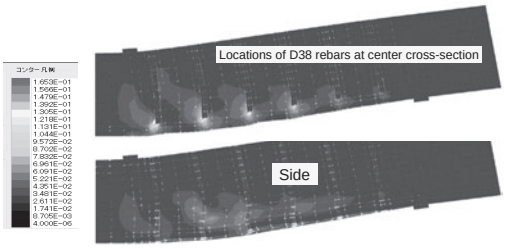

(a) Just before maximum load

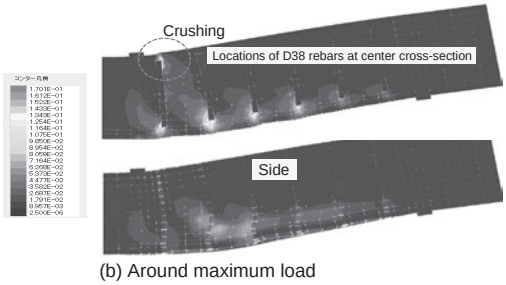

(b) Around maximum load

Fig. 14 Results of Case-3 Specimen Failure Behavior Analysis

6 Conclusion

This study can be summarized as follows.[11]

(1) From the failure tests of RC beams of equal shear reinforcement using two types of shear rebars (D25 and D38), we found that flexural failure occurred with the beam having D25 rebars and compressive shear failure with the beam with D38 rebars.

(2) With D25 rebars, setting the length of the rebar ineffective area as 1.5 times the rebar diameter allowed us to reproduce the failure behavior for the most part.

(3) With large-diameter rebars, the mechanism of compressive shear failure was as follows. At around the maximum load, bonding of large-diameter rebars began to be lost at their upper and lower ends, and stress was concentrated on the compression side. And as crushing occurred, shear cracking went through the upper edge of the specimen and resulted in failure.

Reference:

1) Takaki Kato, Teruki Aoi, "Shin-chitose Kuko ni okeru Doboku Shisetsu no Taishin Taisaku ni tsuite [in Japanese]", *Report at the 9th Airport Technology Workshop* (December 2008)

2) Susumu Okamoto, Tatsuo Mioke, Ken-ichi Horiguchi, Tohru Fukawa, Motoshi Chujyo, Kouichi Kanou, "Development of Post Shear Reinforcing Methods Using Plate-Anchored Shear Reinforcing Bar Technology", *Report of Taisei Technology Center,* No. 40, TAISEI Corporation (2007)

3) Koichi Tanaka, Joji Ejiri, "Out-of Plane Shear Reinforcing Method "Multiple Nuts Bar" for the walls of Underground RC Structures", *Report of Obayashi Corporation Technical Research Institute,* No. 74, Obayashi Corporation (2010)

4) Yoshihisa Kanamitsu, Kosuke Furuichi, Shinichi Yamanobe, Naoki Sogabe, Akitoshi Ishii, Hiroaki Kougami, Masaaki Ueda, Takeshi Sanuki, "Development and Application of a Seismic Retrofitting Method Using Ceramic Cap Bars in Underground Reinforced Concrete Structures", *Kajima Technical Research Institute Annual Report,* No. 59, Kajima Corporation (September 30, 2011): 29 - 36

5) Kensuke Yamamura, Osamu Kiyomiya, "Earthquake-Proof Reinforcement by Steel Inserting Method on Shear Force for Wall of Excavation Structure [text in Japanese]", *Proceedings of JSCE,* No. 777 / VI-65, Japan Society of Civil Engineers (December 20, 2004): 37 - 51

6) Ken'ichiro Nakarai, Hai Le Duyen, Koichi Maekawa, "Risan Haichi Hokyokin ni yoru Kisetsu RC Buzai no Sendan Hokyo Koka [in Japanese]", *Proceedings of JSCE E,* Vol. 63, No. 1 (February 2007): 116 - 126

7) Hajime Okamura, Koichi Maekawa, *Tekkin Concrete no Hisenkei Kaiseki to Koseisoku* [in Japanese], Gihodo Shuppan Co., Ltd. (May 1991)

8) Koichi Maekawa, Hikraru Nakamura, Yasuhiko Sato, Kukrit Toongoenthong, "Sendan Hokyokin no Teichaku Furyo ga RC Hari no Sendan Tairyoku ni Oyobosu Eikyo [in Japanese]", *Proceedings of the Japan Concrete Institute,* Vol. 26, No. 2, Japan Concrete Institute (2004): 973 - 978

9) *Standard Specifications for Concrete Structures – 2007, "Design", JSCE Guidelines for Concrete No. 15*, Japan Society of Civil Engineers (December 2010)

10) Tetsuya Mishima, Buja Bujdham, Koichi Maekawa, Hajime Okamura, "Tekkin Concrete Risan Hibiware o Koseisuru Zairyo Model no Kaihatsu [in Japanese]", *Proceedings of JSCE,* No. 442 / V-16, Japan Society of Civil Engineers (February 1992): 171 - 179

11) Kaoru Kobayashi, Hideaki Takano, Naomi Sasaki, "Bojo Sendan Hokyo Tekkin o Haichishita RC Buzai no Sendan Hakai Kyodo ni kansuru Kiso Kento [in Japanese]", *Proceedings of the Japan Concrete Institute,* Vol. 35, No. 2, Japan Concrete Institute (2013): 1,033 - 1,038